Rev. Adv. Mater. Sci. 33 (2013) 436-441

DEFORMATION BEHAVIOR OF THIN-WALLED TUBE BENDING WITH INTERNAL PRESSURE

B. G. Teng, L. Hu and S. J. Yuan

School of Materials Science and Engineering, Harbin Institute of Technology, 92 West Da-Zhi Street, Harbin 150001, China

Received: October 17, 2013

Abstract. To clarify the deformation behavior of thin-walled tube under combined bending and internal pressure, the hydro-bending experiments of aluminum alloy 5A02 thin-walled tubes with internal pressure ranged from zero to 1.33 times of yield pressure of the tube are carried out. Combined with the numerical simulation, the effect of the internal pressure on the section flattening, wall thickness distribution, and the bending limit of the thin-walled tube are studied. It is shown that even a small value of internal pressure enhances the section stiffness of the thin-walled tube and delays the cross-section flattening. The non-circularity decreases rapidly at the beginning and the decrease rate goes down with internal pressure increasing. The stability and the bending limit of the thin-walled tube are improved evidently with internal pressure increasing. The axial compressive stress magnitude at the intrados decreases gradually as the internal pressure increases, which is beneficial to the prevention the instability and winkling defect.

1. INTRODUCTION

In the past decades, the thin-walled elbow parts (D/t>20, D-tube diameter, t-wall thickness) have been widely used in aerospace and automobile industries for their high strength/weight ratio [1]. However, wrinkling and cross-section distortion usually occur in an early stage of the thin-walled tube bending process. Great efforts have been taken to prevent the bending defects and improve the bending limit using various bending processes, including NC rotary draw bending [2-5], filler bending [6], stretch bending [7,8], etc.

The hydro-bending process has been developed to fabricate the thin-walled elbow tubes due to its main advantage of the adjustable internal pressure and the smaller section distortion, as well as the opportunity of integration into the hydroforming process [9]. It was shown by hydro-bending experiments of stainless steel tubes (D/t = 52) that the collapse curvature under the internal pressure of $0.75p_y$ (p_y - yield pressure of the tube) was about six times higher than that without internal pressure. The section distortion was well controlled under higher levels of internal pressure, and a minimum value of relative bending radius ($R'=R/D$, R-centerline bending radius) of 7 was observed [10]. It was shown from a series of hydro-bending experiments on mild steel tubes with D/t = 100 that the increase of internal pressure could delay the onset of wrinkling notably, but the minimum value of relative bending radius still reached 15 under the yield pressure of the tube [11]. Moreover, the results from hydro-bending experiments and numerical simulations of mild steel tubes with D/t = 32.6 showed that the internal pressure could relieve the wrinkling tendency at the intrados by producing an additional tensile stress along the longitudinal direction. The forming limit was improved and a minimum value of relative bending radius of 5 was obtained [12].

In present study, a series of hydro-bending tests of aluminum alloy 5A02 tubes is performed to investigate the bending behavior and the forming limit

Corresponding author: L. Hu, e-mail: hithl@msn.com

Table 1. Mechanical properties of thin-walled tube.

Material	Aluminum alloy 5A02
Yield strength σ_s (MPa)	79
Tensile strength σ_b (MPa)	175.2
Hardening exponent *n*	0.24
Strength coefficient *K* (MPa)	296
Total elongation at fracture (%)	21.9

under different levels of internal pressure. A 3D elastic-plastic FE model is built up under the ABAQUS/Explicit platform. The effects of the internal pressure on the section distortion, the wall thickness distribution and the bending limit are investigated.

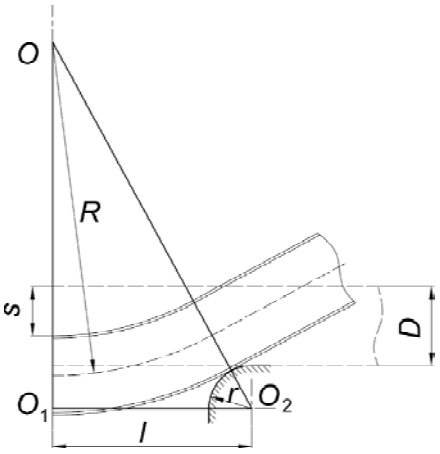

Fig. 2. Diagram of geometrical relationship between upper die displacement and centerline bending radius.

2. MATERIAL AND METHODS

2.1. Material properties

Aluminum alloy 5A02 thin-walled tubes were used in the present study. The outer diameter of the bending specimens was 63 mm, the wall thickness was1mm, and the tube length was 900 mm. The tubes were in the annealed condition. The average material properties of the tube are given in Table 1, which were obtained from uniaxial tensile tests with specimens cut along the longitudinal direction of the tube. The Hollomon model ($\overline{\sigma} = K\overline{\varepsilon}^n$) was used to describe the strain hardening of the materials, where *K* is the strength coefficient, and *n* is the strain hardening exponent.

2.2. Experimental setup

The experimental setup for hydro-bending tests of aluminum alloy tubes is shown in Fig. 1, which is in the three-points bending form. The upper die moves downward to press the tube against the die cavity. End plugs with the self-tightening structure [11] were employed and the internal pressure was provided by a pump. Moreover, press plates were adopted to restrain the upward displacement of tube ends, which could prevent wrinkling by applying additional tensile stress to the intrados of the tube.

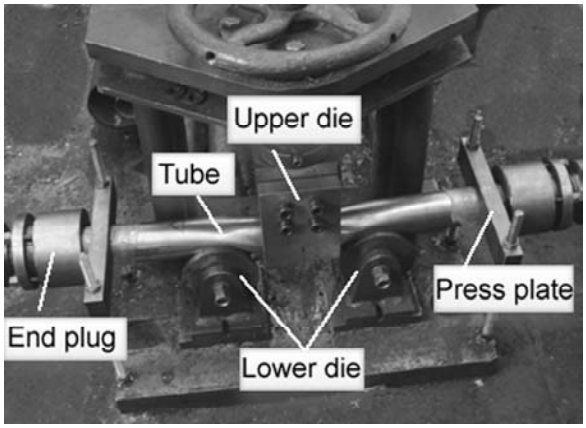

Fig. 1. Hydro-bending experimental setup for aluminum alloy tubes.

The centerline bending radius could be estimated indirectly from the upper die displacement. By applying the Pythagoras Theorem to the triangle OO_1O_2, as shown in Fig. 2, the relationship between centerline bending radius (*R*) and upper die displacement (*s*) could be derived as:

$$R = \frac{l^2 + s^2}{2s} - r - \frac{D}{2}, \tag{1}$$

where, *l* is the distance from O_2 to O_1; *r* is the radius of round corner, and *D* is the initial outer diameter of tube.

As a measure of flattening of the cross-section, the non-circularity is defined as:

$$\delta = \left(OD_{\max} - OD_{\min}\right) / D, \tag{2}$$

where, δ represents the non-circularity of the central section, and $OD_{\max}$, $OD_{\min}$ are the maximum and the minimum outer diameters of the central section, as shown in Fig. 3.

The yield pressure of the thin-walled tube (p_y) could be estimated by the following equation:

$$p_y = \frac{2t}{D}\sigma_s, \tag{3}$$

where, σ_s is the yield strength of the material; *t* is the initial thickness of the tube. According to the

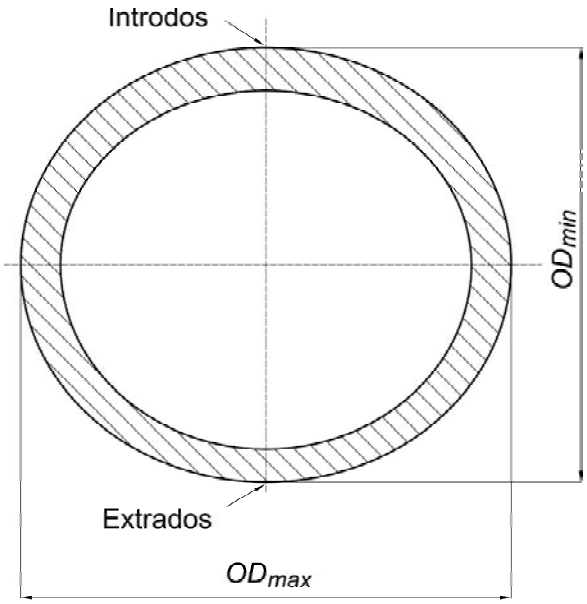

Fig. 3. Diagram of the central section after deformation.

calculated result of the yield pressure, five pressure values including 0 MPa, 0.8 MPa ($0.33p_y$), 1.6 MPa ($0.67p_y$), 2.4 MPa (p_y), and 3.2 MPa ($1.33p_y$) were selected in the present study.

2.3. Finite element model

A 3D elastic-plastic finite element model was established using ABAQUS/Explicit, as shown in Fig. 4. Only a half model was involved into the calculation in view of geometry and loading symmetries. The lower and upper dies and press plates were assumed to be rigid, while the thin-walled tube was modeled with S4R elements, i.e. a 4-nodes quadrilateral shell with reduced integration, with a mesh size of 3 mm and 5 integral points along the thickness direction. The Coulomb friction model with a coefficient of 0.1 was used for all contact surfaces. A constant pressure was applied to the inside of the tube and end caps.

3. RESULTS AND DISCUSSION

3.1. Effect of internal pressure on flattening of central section

Fig. 5 shows the predicted results of deformation behavior and wall thickness distribution of thin-walled tubes when R' = 6. It is shown that even a small value of internal pressure stiffens the cross section of the thin-walled tube and delays ovalization. Severe section distortion is observed without internal pressure when R' = 6. The flattening of cross section is relieved gradually as internal pressure increases. The non-circularity of the central section under $0.33p_y$, $0.67p_y$, p_y, and $1.33p_y$ are 29%, 15.2%, 11.1%, and 8.9%, respectively. Fig. 6 compares the experimental results of bending without internal pressure and bending under p_y. It is seen that the numerical predicted result agrees well with the excremental results. The tube is completely collapsed in the absence of the internal pressure, whereas a sound elbow part is obtained under p_y.

The effect of the internal pressure on the flattening of the central section under different cases of R' is shown in Fig. 7. It is shown that with the same relative bending radius (R'), the non-circularities decline rapidly at the beginning and the rate of the decrease goes down as internal pressure increasing. When R' = 10, the non-circularity under the yield pressure is 6.67%, and the value under 3.2 MPa is 6.3%, as against 32.5% in the absence of the internal pressure. The non-circularity increases when the relative bending radius R' decreases. With a same internal pressure of p_y, the non-circularity is 6.6% when R' = 12, whereby the value is 8.73% when R' = 8.

3.2. Effect of internal pressure on wall thickness distribution

The effect of the internal pressure on the wall thickness of the intrados is shown in Fig. 8a. It can be seen that the thickening ratio of the intrados de-

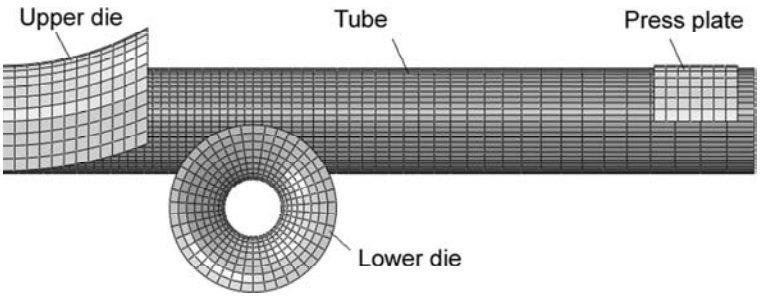

Fig. 4. FE meshes of hydro-bending process.

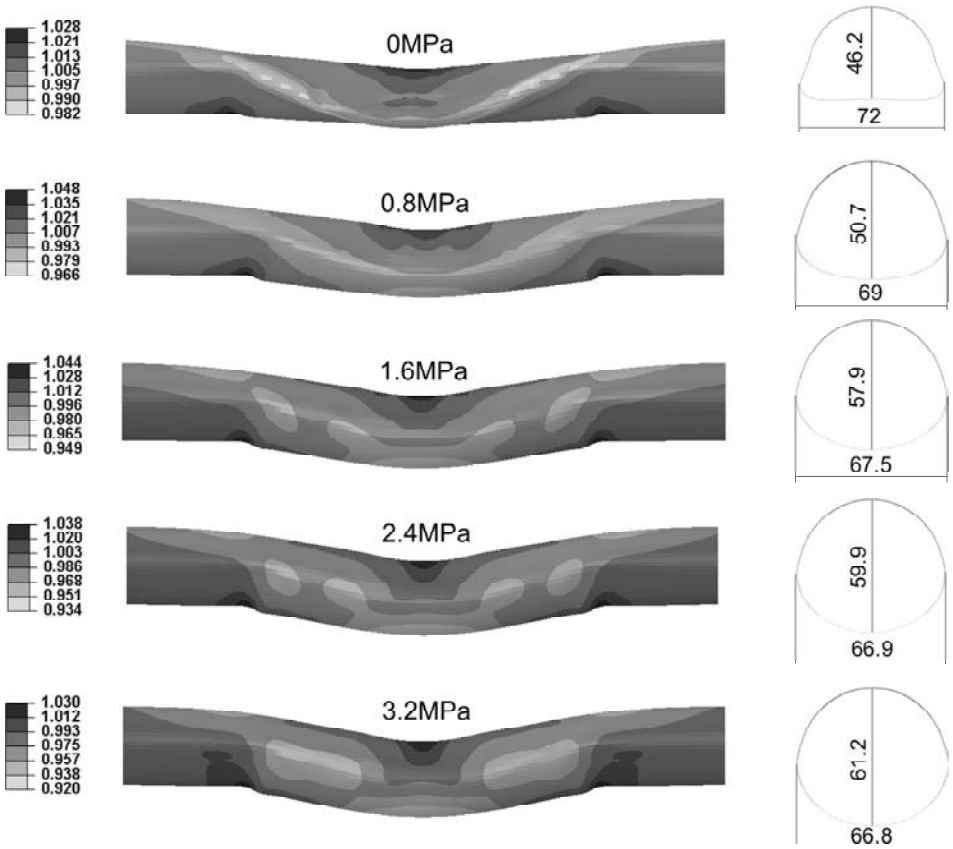

Fig. 5. Numerical predicted deformation behavior and wall thickness distribution of thin-walled tubes when R' = 6 (Unit: mm).

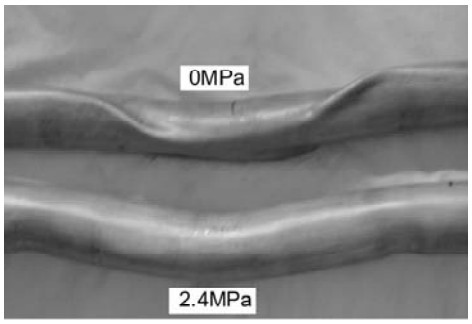

Fig. 6. Experimental results of bending without internal pressure and bending under p_y.

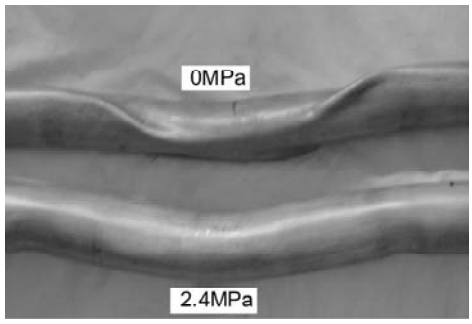

Fig. 7. Effect of internal pressure on non-circularity of central section.

clines with internal pressure increasing: when R' = 10, the thickening ratio of the intrados under 2.4 MPa (p_y) and 3.2 MPa ($1.33p_y$) are 6% and 3.4%, as against 15.3% in the absence of the internal pressure. When R' = 8, the thickening ratio of the intrados under p_y and $1.33p_y$ are 6.8% and 6.4%, respectively. The influence of the internal pressure on the wall thickness of the extrados is shown in Fig. 8b. It is clear that the thinning ratio of the extrados increases near linearly as internal pressure increasing. When R' = 10, the maximum thinning ratios are 9% and 12.4% under p_y and $1.33p_y$, as against 2.1% in the absence of the internal pressure. When R' = 8, the thinning ratios of the extrados under p_y and $1.33p_y$ reach 9.4% and 12.8%, respectively. It is also seen from the wall thickness distribution (Fig. 5) that the wall thicknesses decrease as a whole when the internal pressure increases.

3.3. Effect of inner pressure on bending limit of thin-walled tubes

The attainable minimum relative bending radius, under which a defect free part could be obtained, is referred to as the bending limit. Fig. 9 shows experimental results of elbow tube under p_y. As can

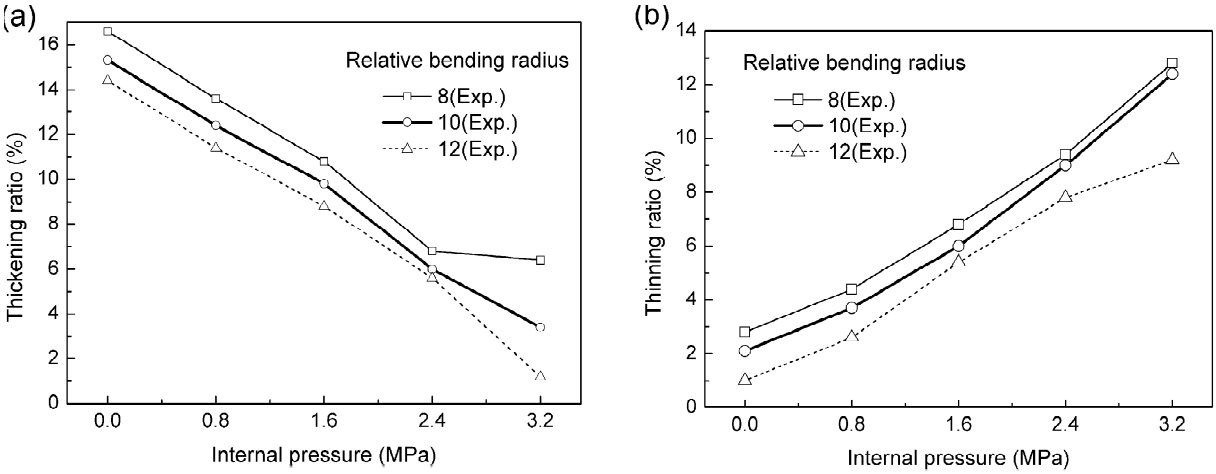

Fig. 8. Influence of internal pressure on wall thicknesses of (a) Intrados and (b) Extrados.

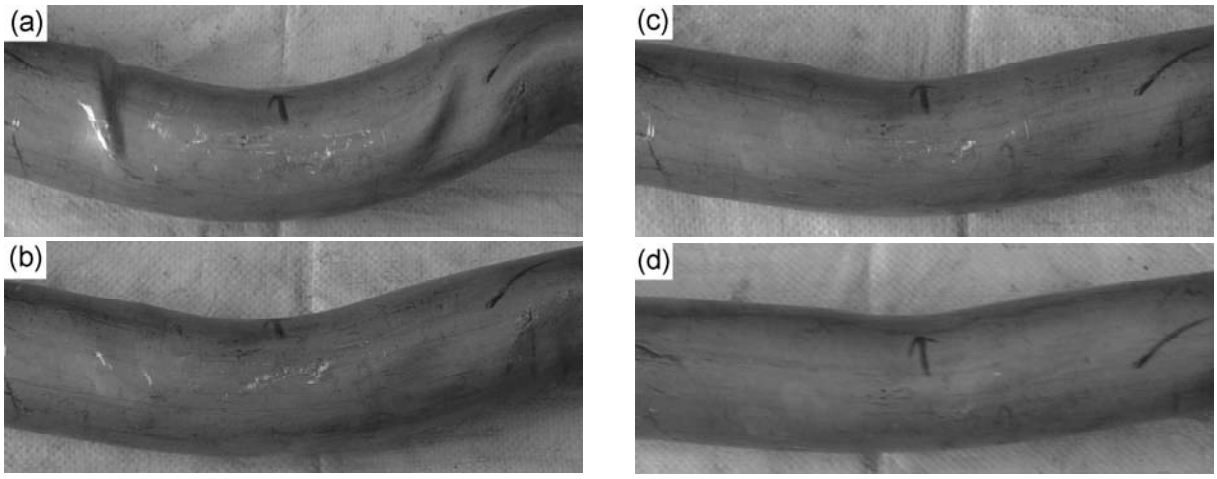

Fig. 9. Results of hydro-bending experiment under the yield pressure with different relative bending radii: (a) R' = 4, (b) R' = 5, (c) R' = 6 and (d) R' = 8.

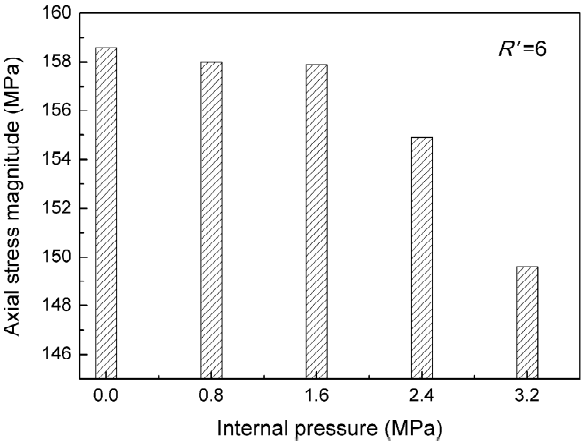

Fig. 10. Effect of internal pressure on axial stress magnitude of intrados.

be seen, a sound elbow tube without defects is obtained when R' = 6. It is shown that internal pressure enhanced the bending stability and increases the bending limit, even at a low level of internal pressure. The bending limit under $0.33p_y$, $0.67p_y$, and $1.33p_y$ are 10, 8, and 6, respectively. However, the value without internal pressure support is around 25. It is noted that the tube diameter is expanded by 3% under $1.33\,p_y$ and there is no evident increase of bending limit.

3.4. Effect of internal pressure on axial compressive stress of intrados

The axial stresses at the intrados play a significant role on the initiation of wrinkling. The effect of the internal pressure on axial compressive stress magnitude at the intrados of the thin-walled tube is shown in Fig. 10. It can be seen that when R' = 6, the axial stress magnitude at the intrados decreases gradually as the internal pressure increases: the value in the absence of the internal pressure is 158.6 MPa, and the axial stress magnitude is 149.6 MPa under $1.33p_y$. The additional axial tensile stress brought by the internal pressure could reduce the degree of compression at the intrados. The decrease of axial

stress magnitude at the intrados is beneficial to the prevention of wrinkling at the intrados during bending.

4. CONCLUSIONS

The bending behavoir of alluminum alloy 5A02 thin-walled tubes in the presence of the internal pressure is investigated experimentally and numerically. The effects of the internal pressure on the section flattening, the wall thickness distribution and the bending limit are analyzed. The following conclusions can been derived:

(1) The section stiffness is enhanced greatly with internal pressure increasing. Section collapse is observed in the absence of the internal pressure, whereas the section flattening is relieved gradually with the increase of the internal pressure. The non-circularity of the central section decreases quickly as the internal pressure increases.

(2) The thickening ratio of the intrados decreases as internal pressure increasing, and the thinning ratio of the extrados ascends near linearly with the increase of the internal pressure.

(3) The stability and the bending limit of the thin-walled tube are improved evidently with internal pressure increasing. The minimum value of relative bending radius decreases with the increase of the internal pressure. The bending limits under the yield pressure and $1.33p_y$ both reach to 6 in the current condition.

(4) The additional axial tensile stress brought by the internal pressure could reduce the degree of compression at the intrados. The magnitude of the axial compressive stress at the intrados declines as the pressure increasing, which is beneficial to the increase of the stability and the forming limit of the thin-walled tube.

ACKNOWLEDGEMENT

The authors would like to thank the National Natural Science Foundation of China (No. 50875060) for the supports given to this research.

REFERENCES

[1] C. Mathon and A. Limam // *Thin-Walled Struct.* **44** (2006) 39.

[2] C. Li, H. Yang, M. Zhan, X.D. Xu and G.J. Li // *Trans. Nonferrous Met. Soc. China* **19** (2009) 668.

[3] H. Li, H. Yang, M. Zhan and Y.L. Kou // *J. Mater. Process. Technol.* **210** (2010) 143.

[4] H. Li, H. Yang, J. Yan and M. Zhan // *Comput. Mater. Sci.* **45** (2009) 921.

[5] H. Li, H. Yang, M. Zhan and R. J. Gu // *J. Mater. Process. Technol.* **187-188** (2007) 502.

[6] M.V. Chitawadagi and M.C. Narasimhan // *J. Constr. Steel Res*. **65** (2009) 1836.

[7] J.E. Miller, S. Kyriakides and A.H. Bastard // *Int. J. Mech. Sci.* **43** (2001) 1283.

[8] E. Corona // *Int. J. Mech. Sci.* **46** (2001) 433.

[9] M. Koc and T. Altan // *J. Mater. Process. Technol.* **108** (2001) 384.

[10] A. Limam, L. H. Lee, E. Corona and S. Kyriakides // *Int. J. Mech. Sci.* **52** (2010) 637.

[11] M. Lovric, In: *Proceedings of the 4th International Conference on Hydroforming*, ed. by M. Liewald (Frankfurt: Werkstoff-Informationsges, 2005), p. 365.

[12] Z.Y. Liu, B.G. Teng and S.J. Yuan // *Journal of Plasticity Engineering* **16** (2009) 35, In Chinese.